

Metabolite Identification via LC-SPE-NMR-MS of the In vitro Biooxidation Products of a Lead mGlu5 Allosteric Antagonist and Impact on the Improvement of Metabolic Stability in the Series

Simona M. Ceccarelli,* Götz Schlotterbeck,* Patrick Boissin, Martin Binder, Bernd Buettelmann, Steven Hanlon, Georg Jaeschke, Sabine Kolczewski, Ernst Kupfer, Jens-Uwe Peters, Richard H. P. Porter, Eric P. Prinssen, Marianne Rueher, Iris Ruf, Will Spooren, Andreas Stämpfli, and Eric Vieira^[a]

Detailed information on the metabolic fate of lead compounds can be a powerful tool for an informed approach to the stabilization of metabolically labile compounds in the lead optimization phase. The combination of high performance liquid chromatography (HPLC) with nuclear magnetic resonance (NMR) spectroscopy and mass spectrometry (MS) has been used to give comprehensive structural data on metabolites of novel drugs in development. Recently, increased automation and the embedding of on-line solid-phase extraction (SPE) into a integrated LC-SPE-NMR-MS system have improved enormously the detection limits of this approach. The new technology platform allows the analysis of complex mixtures from microsome incubations, combining low material requirements with relatively high throughput. Such characteristics make it possible to thoroughly characterize metabo-

lites of selected compounds at earlier phases along the path to lead identification and clinical candidate selection, thus providing outstanding guidance in the process of eliminating undesired metabolism and detecting active or potentially toxic metabolites. Such an approach was applied at the lead identification stage of a backup program on metabotropic glutamate receptor 5 (mGlu5) allosteric inhibition. The major metabolites of a lead 5-aminothiazole-4-carboxylic acid amide **1** were synthesized and screened, revealing significant in vitro activity and possible involvement in the overall pharmacodynamic behavior of **1**. The information collected on the metabolism of the highly active compound **1** was pivotal to the synthesis of related compounds with improved microsomal stability.

Introduction

Direct coupling of HPLC, MS, and NMR has been used most extensively for the identification of drug metabolites, from both in vivo and in vitro models of human metabolism. Such studies generally reach a high level of detail and relevance when applied to compounds at the discovery-development interface, in clinical phases, or for the detection of minor or potentially toxic metabolites of marketed drugs.^[1]

The emergence of high throughput and reliable in vitro models of metabolism, as well as the enormous improvement of detection limits brought about by modern NMR and MS technology have very much reduced the time and material costs of a thorough metabolite identification study. The application of on-line storage and concentration of eluates from LC, such as the recently described solid-phase-extraction (SPE) technology,^[2] has further incremented the material efficiency and quality of the spectra achievable from crude mixtures of metabolites from subcellular and cellular matrixes.^[3] At present, extensive metabolic studies are feasible also during the discovery phase, for example, to identify extensive and undesirable

metabolic instability in lead series or when there is a suspicion of bioactive or toxic metabolites intrinsic to certain structural features during the hit-to-lead process.

In the course of a program for the identification of a backup series of allosteric antagonists of the metabotropic glutamate receptor type 5 (mGlu5),^[4] we were faced with a selection of highly active in vivo but metabolically unstable compounds. Despite extensive optimization, metabolic stability in rat and

[a] Dr. S. M. Ceccarelli, Dr. G. Schlotterbeck, P. Boissin, M. Binder, Dr. B. Buettelmann, Dr. S. Hanlon, Dr. G. Jaeschke, Dr. S. Kolczewski, Dr. E. Kupfer, Dr. J.-U. Peters, Dr. R. H. P. Porter, Dr. E. P. Prinssen, M. Rueher, I. Ruf, Dr. W. Spooren, Dr. A. Stämpfli, Dr. E. Vieira
Pharmaceuticals Division, F. Hoffmann-La Roche AG
4070 Basel (Switzerland)
Fax: (+41)61-688-6459 (S.M.C.)
Fax: (+41)61-688-7408 (G.S.)
E-mail: simona_m.ceccarelli@roche.com
goetz.schlotterbeck@roche.com

Supporting information for this article is available on the WWW under <http://www.chemmedchem.org> or from the author.

human microsomes remained medium to low for most compounds studied. On the other hand, many compounds showed activity in standard rodent models of anxiety (Vogel conflict and stress-induced hyperthermia (SIH tests))^[5] at remarkably low doses. The 5-aminothiazole-4-carboxylic acid amide **1** (Figure 1) is a good example of the overall profile of the

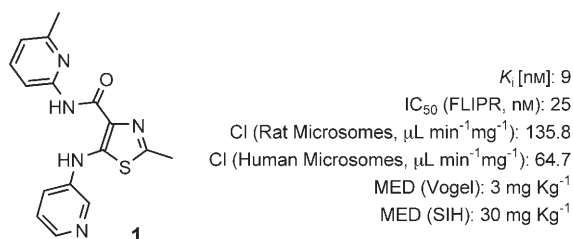


Figure 1. Structure and properties of lead **1**, a mGlu5 Allosteric Antagonist.

series.^[6] The low microsomal stability of **1** in rat microsomes was confirmed by a high intrinsic in vivo clearance in the rat. This made it even more surprising that the compound showed activity in in vivo models of anxiety at a minimal effective dose as low as $\leq 3 \text{ mg kg}^{-1}$ p.o. The identification of the metabolites of **1** had therefore a double interest: a) by elucidating the exact regiochemistry of the biooxidative process, a more informed approach to blocking the most aggressive metabolism could be made available; b) the surprisingly high in vivo activity combined with high clearance suggested the possible involvement of active metabolites in the overall pharmacodynamic effect. In the following, the complete structural characterization of all major metabolites of **1** from human liver microsomes by means of LC-SPE-NMR-MS, involving both one- and two-dimensional NMR, is described, starting from a sample of only $\sim 30 \text{ mg}$ of parent compound. The major metabolites detected were synthesized and confirmed to be highly active as antagonists at the mGlu5 receptor. Moreover, the information gathered on the exact regiochemistry of biooxidation allowed targeted modifications of the parent **1** which led to much more stable compounds in the same series with comparable efficacy, thus reducing the possibility of active metabolites contributing to the pharmacodynamic effect.

Results and Discussion

Metabolite identification by MS/MS analysis

A standard and reliable method for the assessment of metabolic pathways in preclinical phases is the preincubation with microsomes followed by MS/MS analysis of the mixture of metabolites formed.^[7] This allows elucidation of both number and amount of metabolites as well

as the generation of sensible hypotheses regarding their proposed structures. The value and scope of the information provided by such methods is the result of several factors, including extent of metabolism, retention time, and ionization behavior of the products formed, and the extent and diagnostic value of the fragmentation patterns of each metabolite. Typically, very reliable information can be obtained on the regions of the molecules which are the main target of oxidative metabolism, but only in rare cases a precise identification of the structure of the metabolites can be obtained. The MS/MS analysis of the supernatant of the incubation of **1** with human liver microsomes is a typical example. Five major metabolites were identified and a raw outline of the general oxidative pathways was provided, pointing at single and double oxidation at all three heteroaromatic rings, with possible involvement of side-chain oxidation of the methyl group on the pyridine ring (Figure 2).

As we were interested in elucidating the involvement of active metabolites in the in vivo pharmacology of **1**, precise structural information on metabolites was desirable, so as to evaluate possible synthetic approaches and eventual testing of such molecules in vitro and in vivo.

Metabolite identification by LC-SPE-NMR-MS

After screening the panel of 14 recombinant human CYP450 enzymes and comparison of the metabolite profiles obtained to that of human liver microsomes, three isozymes (1A2, 2C18, and 2D6) were chosen that gave the highest biotransformation yields for the respective metabolites. Although CYP3A4 produced all the metabolite peaks seen in human liver microsome incubations, the specificity and biotransformation yield was much less good than in the three isozymes chosen for preparative reactions. In the case of CYP1A2, two metabolites were formed: one was produced within a very short incubation time, whereas the second one needed much longer. For this reason, two separate incubations with CYP1A2 were carried out, so as to access separately both metabolites. To obtain sufficient amounts of metabolites for spectral characterization, 6.5 mg amounts of compound **1** were incubated separately

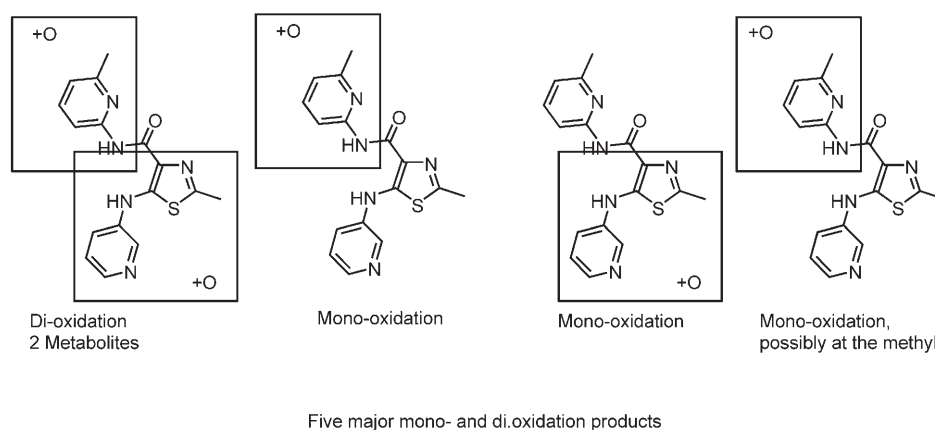


Figure 2. Putative metabolic pathway from MS/MS analysis of incubates of **1** in liver microsomes.

with whole recombinant *E. Coli* cells containing human CYPs 1A2, 2C18, and 2D6 and co-expressing P450 reductase.^[8] After 24 h incubation at 27 °C, the biomass-free supernatant was collected, concentrated, and submitted to LC-SPE-NMR-MS analysis.

Today, LC-SPE-NMR-MS is the state-of-the-art technique for fast structural characterization of mixtures. LC-SPE-NMR-MS is the logical enhancement of LC-NMR that expands the applications of this hyphenated technique significantly.^[2] A general scheme for LC-SPE-MS-NMR coupling is depicted in Figure 3A.

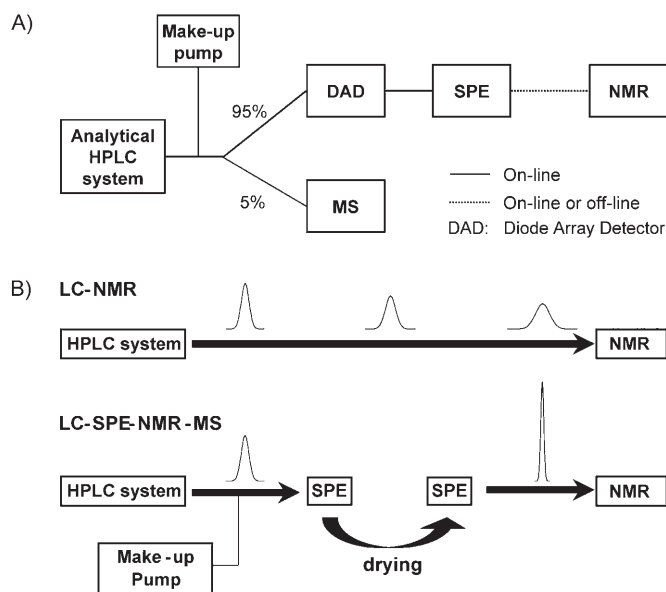


Figure 3. A) General Scheme for LC-SPE-MS-NMR. B) Enrichment of chromatographic peaks in LC-SPE-MS-NMR compared to conventional LC-NMR.

The chromatographic flow is split after the separation in two parts. The major proportion is directed to the SPE device for enrichment and subsequent on-line or off-line NMR analysis. The minor part of the chromatographic flow is guided into the MS spectrometer. A make-up pump that delivers water to the chromatographic flow ensures retention on the SPE cartridge packing material for peak trapping. Figure 3B illustrates the beneficial enrichment and chromatographic peak sharpening effect of the post-column SPE approach. Chromatographic peak broadening as observed in LC NMR is avoided. Trapped peaks can be easily eluted with sharp elution profiles with deuterated organic solvents.

LC-SPE-NMR-MS offers significant advantages compared to conventional LC-NMR: 1) in analysis of complex mixtures one is often faced with samples where additional MS information guides LC-NMR to decide whether the UV-monitored LC-peak is the peak of interest; 2) the simultaneous acquisition of MS and NMR spectra from the same chromatographic peaks from one sample allows a structure to be delineated where MS and NMR data alone would not be sufficient; 3) the LC separation cannot be exactly reproduced in different laboratories or different instruments so that MS and NMR spectra are not safely attributable to one and the same chromatographic peak. This sit-

uation often happens and severely hampers structure determination; 4) on-line post column enrichment of chromatographic peaks by SPE dramatically reduces the NMR measuring times (see Figure 3B). This is especially the case for trapping corresponding peaks of repeated injections onto the same SPE cartridges. Chromatographic peak broadening effects in LC-NMR by use of long capillary connections and the large volume of the NMR flow-cell are circumvented; 5) chromatographic conditions (solvents, buffer etc) can be freely chosen. No need for replacement of H₂O by D₂O as in conventional LC-NMR is needed. Protonated solvents can be easily removed by the drying procedure on the SPE cartridge. The enriched compound is then eluted with a small volume of deuterated organic solvent for example, [D₃]acetonitrile either directly on-line via a capillary into the NMR flow cell or off-line into a NMR tube.

Hence, LC-SPE-MS-NMR coupling is an extremely important technique for valuable, mass limited samples. Laborious serial isolation and purification procedures of metabolites, byproducts, or impurities from complex biomatrices or chemical reactions can be circumvented by use of an integrated system. Thus purified product in amounts sufficient for structure elucidation by NMR and MS can be obtained much faster and easier.

Figure 4 exemplifies the amount and quality of the spectral information obtainable by this procedure. Due to the high concentration of the sample eluted from SPE cartridges and the use of deuterated solvents, it is possible to obtain in reasonable experimental time not only high quality one-dimensional spectra (see Figure 4A, with metabolite **2** as example), but also two-dimensional spectra (Figure 4B and C). This allows unambiguous assignment of the structure, with the MS analysis offering confirmatory evidence.

Figure 5 shows a UV-chromatogram from HPLC analysis of an incubation of **1** with human liver microsomes, showing the five main metabolite peaks together with the unambiguous structural assignment of each peak to compounds **2–6**, following LC-SPE-NMR-MS analysis.

Surprisingly, the main metabolite from microsomal oxidation emerging from this characterization effort was not, as expected, the product of oxidation at one of the methyl side chains, but the phenol **3** resulting from oxidation in position 5 of the pyridine ring, adjacent to the methyl group. The second most prominent metabolite **2** was, as foreseen by the MS/MS analysis, the product of hydroxylation of the methyl group alpha to the pyridine nitrogen.

Chemistry

The synthesis of **2** and **3** was performed as indicated in Scheme 1. 3-Hydroxy-2-methyl pyridine **8** was subjected to nitration conditions yielding a 3:1 mixture of nitrated isomers **9** and **10** respectively. Unfortunately the desired 6-nitro isomer **10** was the minor one. This was processed to the protected derivative **11** using standard acetylation conditions, and the nitro group was reduced to give the amine **12** by hydrogenation with Pd/C as catalyst. Reaction of this aromatic amine

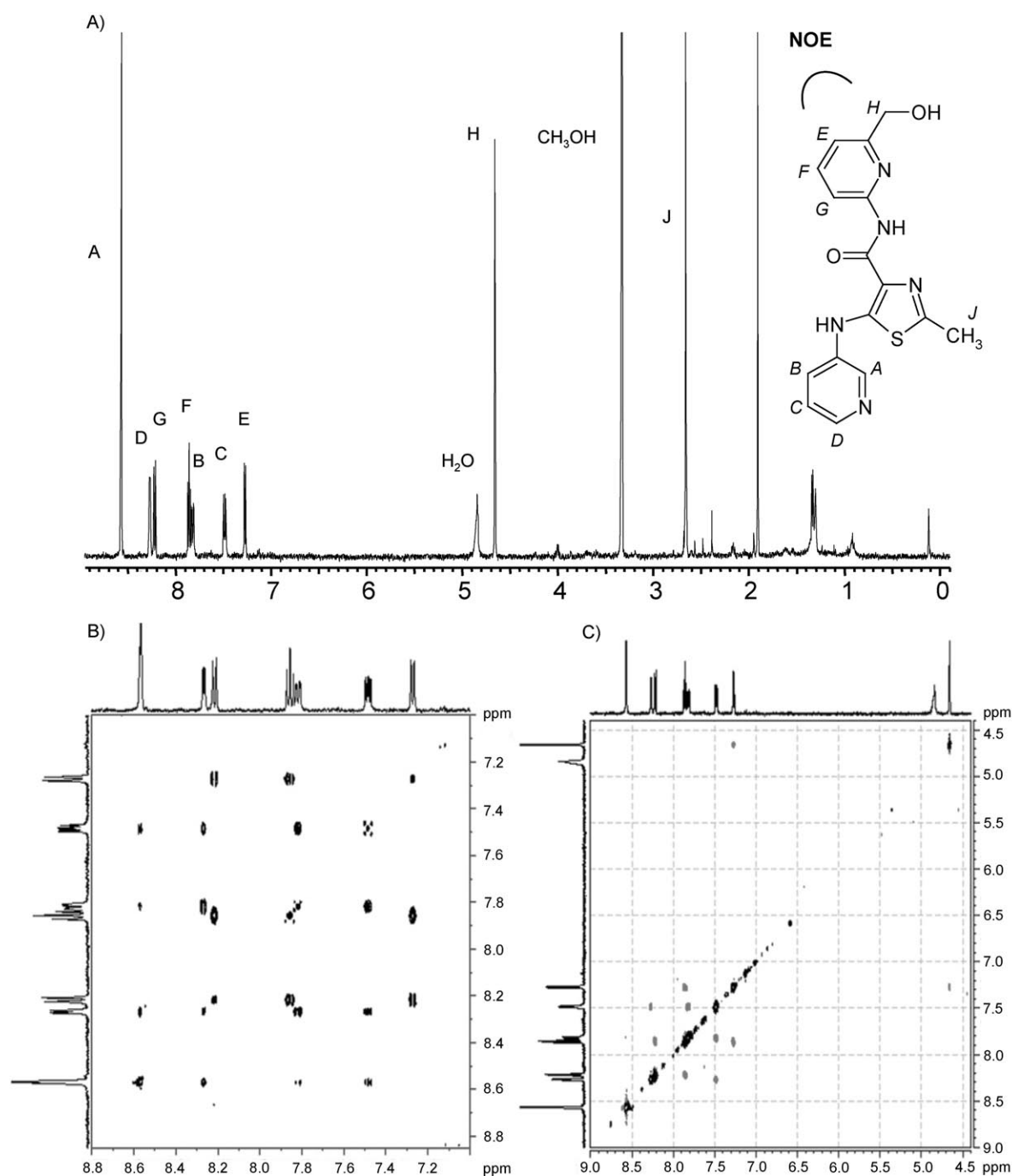


Figure 4. Example of NMR and MS spectra after LC-SPE-NMR-MS and assignment of the structure of metabolite **2**. A) ¹H NMR spectrum at 600 MHz; B) TOCSY; C) NOESY.

with the acyl chloride resulting by treatment of thiazole acid **13** (prepared by treatment with elemental bromine of the corresponding lithiated derivative, obtained by reaction of 2-methyl-1,3-thiazole-4-carboxylic acid with butyl lithium) with thionyl chloride yielded functionalized bromothiazole **14**. Reaction with 3-amino-pyridine **15** under optimized palladium catalyzed coupling conditions (Pd_2dba_3 , Xantphos, and CsCO_3 in dioxane) and microwave irradiation, followed by deprotection of the acetyl group afforded the desired metabolite **3** in sufficient yield.

Synthesis of the hydroxymethyl metabolite **2** was performed starting from the monoester of pyridine 2,6-dicarboxylic acid **16**, which was converted to the protected amine **17** via standard Curtius rearrangement conditions in the presence of *tert*-butanol. The ester group of **17** was reduced to the corresponding hydroxymethyl group with sodium boron hydride in the presence of calcium chloride, followed by acetylation to yield the orthogonally protected derivative **18**. Deprotection of the amino group and coupling with acid **13** yielded the bromothiazole **19**. In analogy to what is described above for the

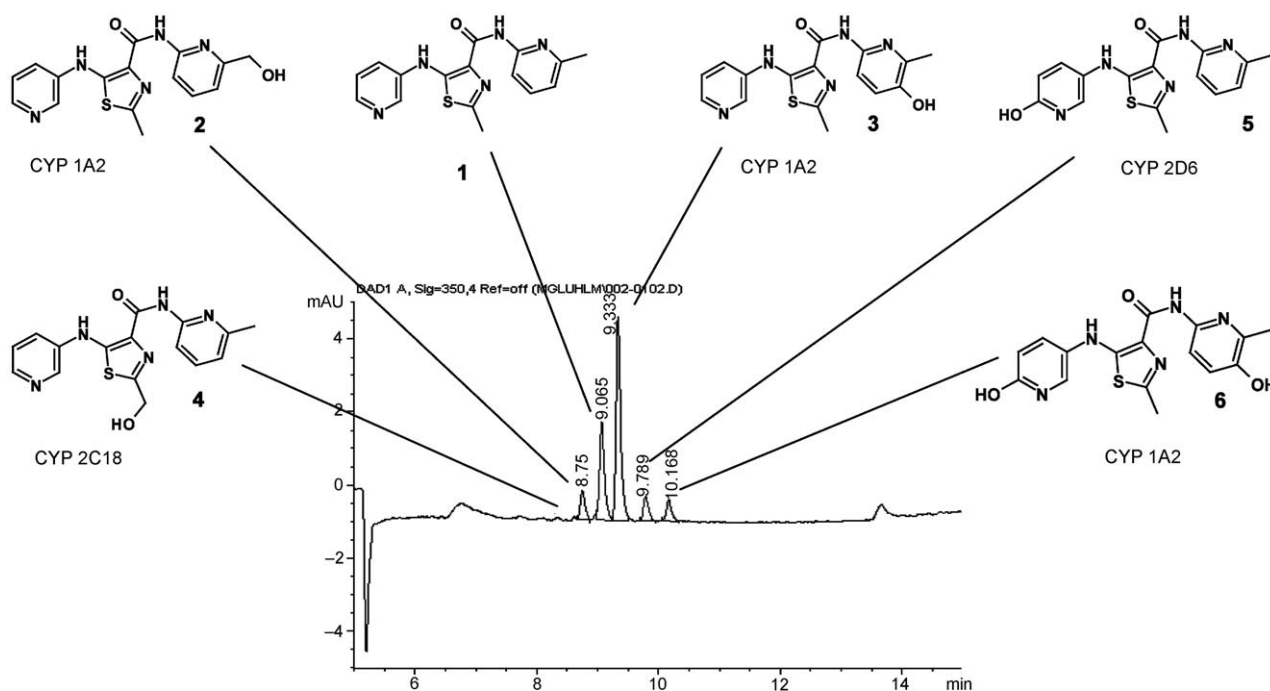
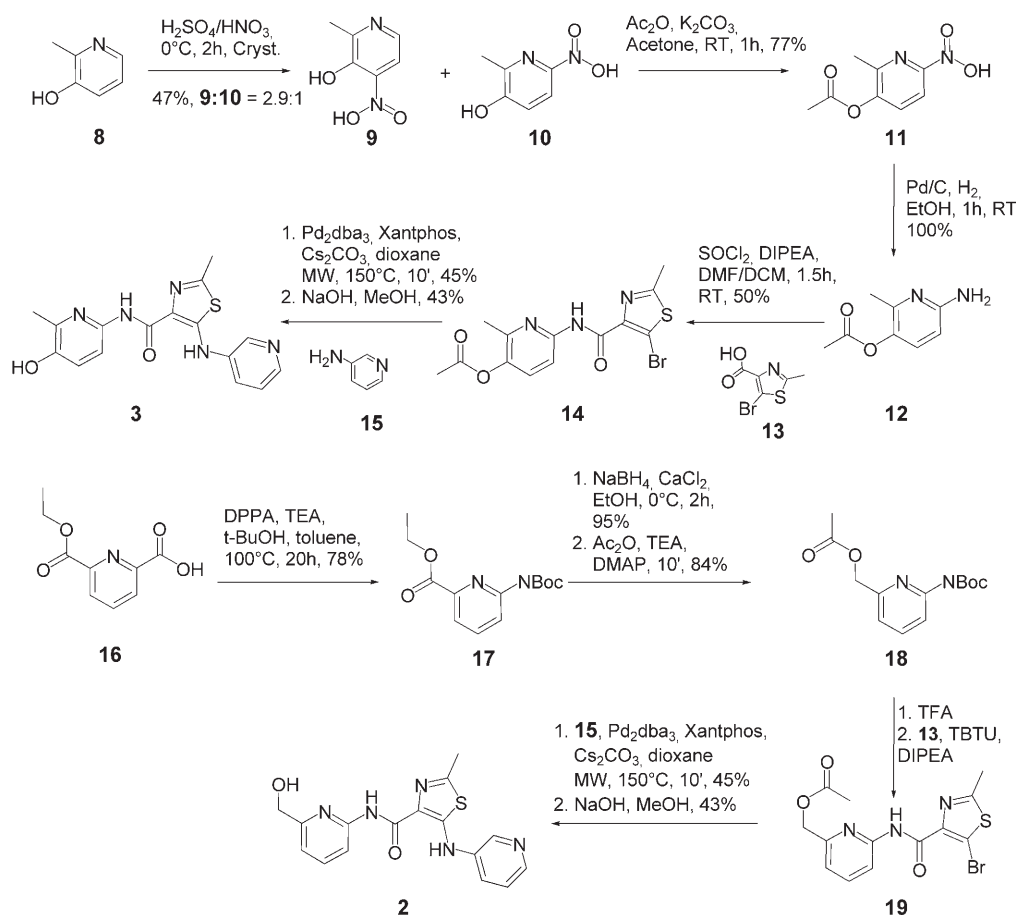


Figure 5. Metabolite profile of compound **1** following HPLC analysis of a human liver microsome incubation. Five main metabolites are formed, corresponding to the structures **2–6**. The CYP isoform which is mainly responsible for the formation of each metabolite is also indicated. Assignment of peaks was done on basis of NMR data.



Scheme 1. Synthesis of the main metabolites of **1** identified by LC-SPE-NMR-MS.

synthesis of **3**, palladium catalyzed coupling with 3-amino-pyridine **15** and final deprotection of the alcohol afforded the desired compound **2**.

Both main metabolites of **1**, bind to the mGlu5 receptor and show functional activity in the FLIPR assay (Table 1), albeit **3** is

tion of **1** are the positions *para* to the amine substituents on both pyridine rings as well as the methyl group of the methylpyridine, as indicated by the arrows in Figure 6. No, or very limited oxidation takes place on the thiazole methyl, whereas there is no evidence of involvement of the other aromatic C-H

groups in the molecule. Although we were aware of the versatility of the metabolizing enzymes, we reasoned that blocking any or all of these positions might be a good initial approach to limiting intrinsic clearance in the series. To this aim, we designed a series of compound **20–24**, as shown in Figure 6. In **20** and **21**, the oxidation in the *para* position of the methylpyridine ring is not possible, and it is to be expected that the kinetics of methyl functionalization in **20** should be changed, as the basic pK_a of the pyridine nitrogen is predicted to increase considerably.

In compound **22**, the oxidation at the position corresponding to the *para* position of the 3-aminopyridine ring of **1** should be notably slowed down, because of the reduced electron density at this site in the pyrimidine ring. Compounds **23** and **24**, finally, combine protection of all three metabolically labile positions.

Synthesis of compounds **20–24** was performed according to the same protocol used for the synthesis of **1** and is illustrated in Scheme 2.

Aminothiazole **26** was prepared starting from ethyl acetamidocynoacetate **25** by treatment with Lawesson's reagent.^[9] Reaction of the amino group of **26** with aryl bromide under palladium catalysis and similar conditions as described for the synthesis of **2** and **3** yielded intermediates **27** and **28** respectively. These ethyl esters were coupled with the desired pyridine amine-trimethylaluminum complexes, allowing access to the compounds **20–24**. Compound **1** was prepared from the acid **29** by standard TBTU promoted amide formation with 6-amino-2-picoline. As predicted, the basic pK_a of the methylpyridine nitrogen of compounds **20** and **24** is close to physiologi-

considerably less active than **1** (approximately one order of magnitude). Although both **2** and **3** by themselves do not show efficacy in the Vogel's model of anxiety up to 10 mg/Kg after p.o. administration, it cannot be a priori excluded that they do not contribute to the pharmacological activity of **1**, as they are formed after absorption of **1** has taken place and may reach higher local exposures in the course of the in vivo processing of **1** than is possible by direct administration in the gastrointestinal tract. Intrinsic clearance rates of **2** and **3** are slightly lower than for **1** in both rat and human liver microsomes.

The precise information on the sites of oxidative metabolism of **1** offered the possibility of a rational approach to the generation of metabolically stable analogues. Provided comparable or superior efficacy in our selected in vivo model is reached, compounds with reduced intrinsic clearances would have a reduced risk for the involvement of active metabolites. This would allow a clearer understanding of the relationship between pharmacokinetic and pharmacodynamic effect, which is essential for a reliable allometric scaling. As apparent from the analysis detailed above in Figure 4, the main sites of biooxida-

Compd	K _i [nM] ^[a]	IC ₅₀ [nM] ^[b]	Cl (RM) [uL min mg ⁻¹] ^[c]	Cl (HM) [uL min mg ⁻¹] ^[c]	MED [mg Kg ⁻¹] ^[d]
1	10	31	135.7	64.8	3
2	67	105	88.9	34.1	> 10
3	111	477	75.2	39.8	> 10
20	44	57	78.9	65.1	3
21	13	17	188.0	43.5	–
22	20	34	123.4	233.5	6
23	31	36	0.0	57.1	–
24	81	130	25.3	38.5	3

[a] Determined by displacement of radiolabeled 2-methyl-6-phenylethynyl-pyridine (MPEP); [b] Functional Assay: Ca⁺⁺ Efflux IC₅₀ (FLIPR); [c] Intrinsic clearance in rat (RM) or human (HM) microsomes; [d] Minimal Effective Dose (MED) p.o. in the Vogel model of anxiety.

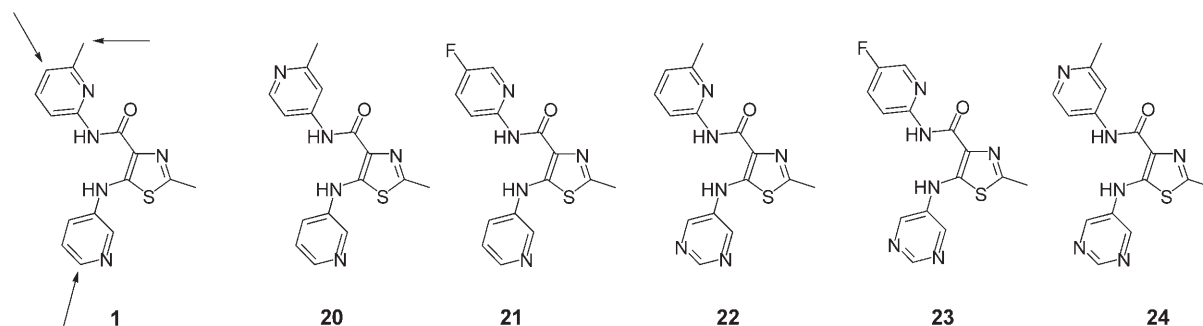
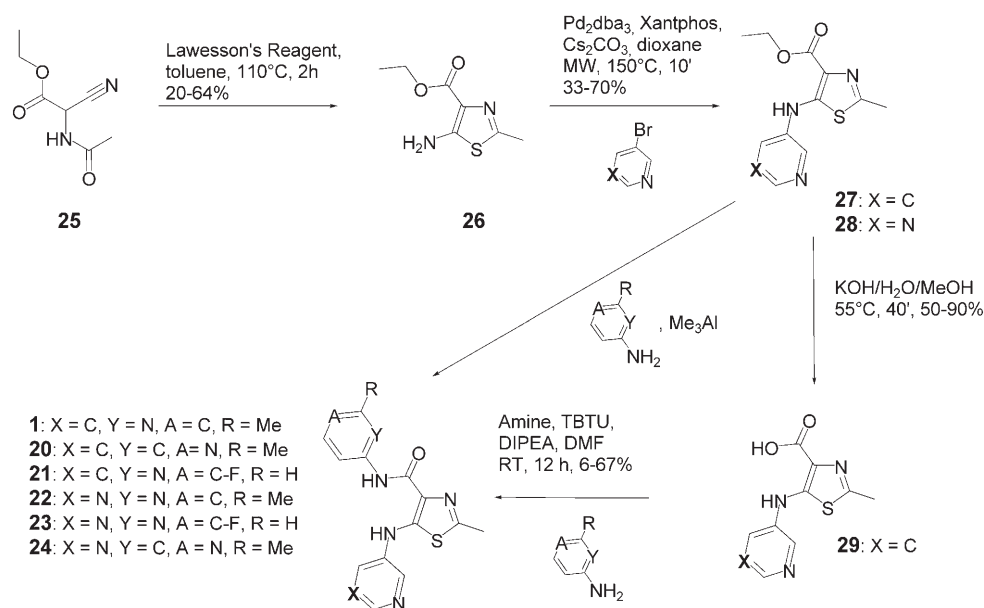


Figure 6. Compounds designed to have reduced metabolic clearance in comparison to **1** by protection of the metabolically labile positions identified on **1**.



Scheme 2. Synthesis of compound 1 and of 20–24.

cal pH ($pK_a=6.6$ for **24**), whereas it is more than two units lower in **1** and **22** ($pK_a=4.25$ for **22**).

In Table 1, the relevant parameters for compounds **20–24** are reported and compared to compound **1**. All compounds show binding and functional activity at the mGlu5 receptor comparable to **1** or only slightly inferior. Protection of only one of the metabolically labile positions does not appear to be sufficient to achieve a notable reduction in the clearance rates in rat liver microsomes, as visible for compound **20** where the 3-pyridylamino moiety is susceptible to metabolic attack or for compound **22** where the most labile 5-position of the 2-amino-6-methylpyridine moiety is still present whereas some improvement can be obtained for human liver microsomes with compound **21** where position-5 is blocked with a fluorine atom. Structural changes at both of these labile positions appears to be more successful. In compound **23**, clearance is blocked in rat liver microsomes, but is still considerably fast in human liver microsomes. Introduction of a fluorine atom at position 5 slowed down metabolism but was not sufficient to completely block it. The fluorine atom in position 5 is activated by the 2-amino group *para* to it which leads also to formation of 5-hydroxy metabolites. Compound **24**, on the other hand, where the carbon atom at position 5 is replaced with a nitrogen atom, and which additionally has the more stable pyrimidine moiety shows reduced clearance rates in both rat and human liver microsomes compared to **1**. The minimal effective dose for this compound in the Vogel model of anxiety is the same as for **1** after p.o. administration, despite a somewhat reduced functional activity at the mGlu5 receptor. It is to be assumed that the involvement of active metabolites as contributors to the pharmacodynamic effect is less likely in the case of **24** than for **1**.

Conclusions

Solid phase extraction technology as applied to characterization of minute amounts of analytes can be a very powerful method for the identification and structural characterization of metabolites of drug candidates and lead structures. The application of on-line storage and concentration of eluates from liquid chromatography allows acquisition of very high quality one- and two-dimensional NMR spectra of each component of complex mixtures of metabolites derived from standard incubation protocols of subcellular and cellular matrixes, even if relatively small amounts of parent compound are employed. We described the application of this concept to the elucidation of the metabolic pathways of a representative allosteric mGlu5 antagonist **1** from a lead series of thiazole-4-carboxylic acid amides.^[6] The compound showed high *in vivo* efficacy in standard models of anxiety despite a very poor *in vitro* and *in vivo* metabolic stability, leading to the assumption that active metabolites might be involved in the pharmacodynamic effect. Incubation of the compound with different CYP enzymes followed by analysis of the mixtures by LC-SPE-NMR-MS allowed precise characterization of all major metabolites, which could be readily synthesized. It could be confirmed that the main metabolites of **1** show considerable activity at the target, thus supporting the hypothesis that the observed *in vivo* efficacy might be due to overlay between the effect of **1** and that of its degradation products. Moreover, as the major sites of metabolism could be identified, a number of derivatives were designed where biooxidation of the former labile positions was made difficult or impossible. Some such compounds, as for example **24**, show indeed a reduced *in vitro* metabolism compared to **1**. Knowledge about the exact structure of the metabolites of **1**, therefore, led to a twofold advantage: 1) the poten-

tial involvement of active metabolites in the pharmacology of **1** could be confirmed and 2) a more informed approach to blocking the most labile sites of metabolism became possible, which led to the design and synthesis of more stable analogues. In general, we believe that the relatively modest time and material requirements for this type of analysis make it possible to perform extensive metabolic studies also in early pre-clinical phases, where issues such as excessive metabolic instability, toxicity flags of unclear relevance or inconclusive relationship between pharmacokinetic and pharmacodynamic effects need to be solved.

Experimental Section

MS/MS analysis of metabolic incubations in human microsomes

Conditions for incubation: Incubation of **1** was performed at a concentration of 10 μM at a total incubation volume of 200 μL containing 0.1 M phosphate buffer pH 7.4, NADPH-regenerating system, and a pool of human liver microsomes purchased from Gentest (20 mg protein/mL) diluted to a final protein concentration of 0.5 mg mL^{-1} in the incubation mixture. The enzymatic reaction was stopped by addition of 600 μL methanol for protein precipitation. Samples were prepared for three different time points: $t=0$ (incubation start), $t=15$ min, and $t=30$ min.

Sample preparation and analytics: Samples were centrifuged for 10 min at 10000 rpm. A sample volume of 50 μL was injected into a 100 μL loop of a reversed phase HPLC system consisting of a CTC PAL HTS autosampler with cooled sample stack and conventional 6-port injector valve (CTC Analytics, Zwingen Switzerland), two Shimadzu LC-10ADvp pumps as binary high pressure gradient system, and a Micromass Quattro Ultima mass spectrometer (Manchester, UK) equipped with an electrospray source running under MassLynx 3.5.

Analytics were performed on an Inertsil ODS3 (150 \times 2.1 mm ID, 5 μm ; GL Sciences Inc from Ercatech, Berne Switzerland). A mobile phase of 10 mM formic acid and acetonitrile was used. The flow rate was 0.25 mL min^{-1} . The gradient started from 20% to 80% acetonitrile within 6 min, then up to 90% acetonitrile in 18 min followed by reconditioning. Samples were analyzed first in full scan mode with positive ionization at a cone voltage of 60 V. Mass range was from 100 to 600 Da to get the complete metabolite pattern. Fragment ion spectra of the detected masses at a collision energy of 25 eV were used to identify the structures of possible metabolites.

Preparation of recombinant *E. coli* biomass

Chemicals: δ -aminolevulinic acid (ALA) was from the Roche inventory. Lysozyme from hen egg white (3.2.1.17) was purchased from Fluka. β -nicotinamide adenine dinucleotide phosphate disodium salt (NADP), D -glucose-6-phosphate disodium salt dihydrate, and glucose-6-phosphate dehydrogenase from yeast, grade 1 were all purchased from Roche Biochemicals. Isopropyl β - D -thiogalactopyranoside (IPTG) was purchased from Senn Chemicals.

Growth media: Two media were used for the growth of recombinant *E. Coli*: Luria Bertani medium (LB) containing 1% Tryptone Peptone (Difco), 0.5% Yeast Extract (Difco), and 1% NaCl. Modified Terrific Broth (TB) (Gillam et al 1993) containing 1.2% Tryptone Peptone (Difco), 2.4% Yeast Extract (Difco), 0.2% Bacto Peptone (Difco), and 0.4% v/v Glycerol. Just before use a phosphate buffer solution consisting of 0.17 M KH_2PO_4 /0.72 M K_2HPO_4 was added (100 mL per L). In addition a trace element solution consisting of the following was added (0.25 mL per L): Fe^{III} citrate (24.5 g L^{-1}), ZnCl_2 (1.31 g L^{-1}), CoCl_2 (2 g L^{-1}), $\text{Na}_2\text{MoO}_4 \cdot 2\text{H}_2\text{O}$ (2 g L^{-1}),

$\text{CaCl}_2 \cdot 2\text{H}_2\text{O}$ (1 g L^{-1}), $\text{CuCl}_2 \cdot 2\text{H}_2\text{O}$ (1.27 g L^{-1}), H_3BO_3 (0.5 g L^{-1}), concentrated HCl (100 mL L^{-1}). When required the antibiotics ampicillin (Na salt) and chloramphenicol were used at concentrations of 50 and 25 $\mu\text{g mL}^{-1}$ respectively.

***E. Coli* CYP450/P450 reductase co-expression strains:** The *E. Coli* CYP450 expressing strains were constructed at the University of Dundee as part of a DTI/LINK program and an overview of the cloning and expression strategy is given in Reference [8]. Three *E. Coli* strains co-expressing P450 reductase with CYP1A2, 2C18, and 2D6 respectively were used for cytochrome P450 production: *E. Coli* JM109 [pCW-ompA.-CYP1A2 + pACYC-pelB-HR], *E. Coli* JM109 [pCW-17 α -CYP2C18 + pelB-HR], *E. Coli* JM109 [17 α -CYP2D6 + pACYC184-pelB-HR]

Recombinant *E. Coli* fermentation: Cells were taken from vials stored in liquid nitrogen and applied to Luria Bertani (LB) agar plates containing the appropriate antibiotic(s). The plates were incubated at 37 $^\circ\text{C}$ overnight. An aliquot of the resulting cells was used to inoculate 500 mL baffled flasks containing 100 mL LB media supplemented with the appropriate antibiotic(s). Following incubation for 18 h at 30 $^\circ\text{C}$ with shaking (150 rpm), the contents of ten such flasks was pooled and used as the inoculum for the 100 L fermentations. Fermentations were carried out in Braun Biotech 150 L vessels with a working volume of 100 L. The growth medium was modified Terrific Broth (Gillam et al 1993) supplemented with the appropriate antibiotic(s) and 0.003% v/v Aseol antifoam. IPTG (1 mM) and δ -ALA (1.0 mM) were added as filter sterilized solutions when the optical density at 600 nm reached 0.6–0.8. The fermentation parameters were as follows: Temperature, 30 $^\circ\text{C}$, stirring 150 rpm, and aeration 0.088 vvm. The duration of the fermentations was typically 24 h. Cells were harvested at 13 000 rpm using a Heraeus 20 RS continuous flow centrifuge. Wet cell mass was estimated by centrifuging in a Sorvall RC3C Plus at 3500 rpm for 30 min. 2 \times TSE buffer (0.1 M Tris-acetate pH 7.6, 0.5 M sucrose, 0.5 mM EDTA) was then added (12.5 mL per 7.5 g wet weight cells) and the pellet resuspended by vigorous stirring. Cell suspensions were shock frozen in dry ice and stored at -80 $^\circ\text{C}$.

Determination of CYP450 content: A volume of fermentation broth (factor F60) in milliliters equivalent to 60 divided by the optical density at 600 nm was centrifuged for 10 min at 10000 rpm in a Heraeus Labofuge III. This ensured that an identical number of cells was used in each determination and allowed assessment of the P450 specific content. The pellet was then resuspended in 2.5 mL TSE buffer and the P450 content determined by CO + reduced - reduced difference spectrometry.^[10] The P450 content of frozen and thawed cells was determined by the same method except that a dilution with 2 \times TSE buffer to give a density of 1 g wet weight cells per 20 mL was made prior to acquiring the CO spectrum.

Biotransformations with recombinant CYP450 containing *E. Coli*.

Frozen cells containing 340 nmoles of the appropriate P450 were thawed and diluted with 0.1 M potassium phosphate pH 7.4 to a density of 1 g wet weight per 4 mL buffer. Lysozyme was then added to a final concentration of 25 μg per mL. The cell suspension was then mixed gently on a roller at 4 $^\circ\text{C}$ for 90 min and spheroplasts were pelleted by centrifugation at 9000 rpm in a Beckmann JA10 rotor also at 4 $^\circ\text{C}$. The pellets were resuspended in a total of 80 mL cold phosphate buffer and stored on ice until required. Biotransformations were carried out in 4 \times 500 mL baffled Erlenmeyer flasks containing 100 mL of 0.1 M potassium phosphate pH 7.4, 20 mL resuspended spheroplasts (80 nmoles P450), and this was supplemented with an NADPH regenerating system consisting of per 100 mL: D -glucose-6-phosphate disodium salt (0.34 g), NADP disodium salt (0.20 g), $\text{MgCl}_2 \cdot 6\text{H}_2\text{O}$ (0.24 g) and glucose-6-phosphate dehydrogenase 0.1 mL (170 Units). Reactions were started

by the addition of the substrate **1** (6.5 mg, 50 μM final concentration). The flasks were incubated at 27 °C on an orbital shaker (220 rpm) typically for 24 h. The progress of the reaction was followed by withdrawing 0.5 mL aliquots and mixing with an equal volume of acetonitrile. Following precipitation on ice for 10 min and centrifugation, the supernatant was analyzed by HPLC as described below.

HPLC for product analysis: HP1100 system; column: Supelcosil ABZ+ Plus, 250 \times 4.6 mm, 5 μm (Supelco no. 5-9197); mobile phase: (A) water, 0.1% TFA; (B) acetonitrile, gradient: 0–12 min: 0% to 48% B; 12–12.1 min: 48% to 0%B; 12.1–17 min: % B; flow rate: 1 mL min⁻¹; detection: 350 nm; ambient temperature; sample: 10 μL ; calibration: external standard of **1**. Quantification of metabolites of **1** was estimated in mg $\cdot\text{equ.L}^{-1}$, assuming the same UV-response factor as for parent compound

Metabolite retention times: Metabolite P2 (8.8 min), P3 (9.3 min), P4 (9.8 min), P5 (10.2 min), **1** (9.1 min).

Preparation of metabolite enriched fractions

The broths were adjusted to pH 2 by addition of concentrated TFA and biomass removed by centrifugation for 20 min at 9000 rpm in a Beckmann JA20 rotor. The recovery of metabolites in the supernatant was in the range 80–100% compared with 40–60% when the pH was not adjusted. The pH of the acidified supernatant was then adjusted to pH 9 by addition of 5 M NaOH. The precipitate formed was removed by filtration. The filtrate was applied to a 10 g C18 column (Varian Megabond Elute) and metabolites eluted with 50 mL steps containing : 0, 10, 20, 30, 40, 50, 60, and 100% acetonitrile in water. Metabolite containing fractions were concentrated by rotary evaporation and after freeze drying submitted for HPLC-NMR-MS analysis.

LC-SPE-NMR-MS analysis

Sample enrichment of the metabolites was achieved with a LC-SPE-MS-NMR system consisting of a Agilent 1100 HPLC system, a Spark Prospekt 2 solid phase extraction system, a Bruker Esquire 3000+ MS instrument equipped with an electrospray interface, and a Bruker AV 600 spectrometer equipped with a 5 mm TCI cryo probe. The chromatographic system was controlled by Hystar 3.0 (Bruker Biospin GmbH, Rheinstetten, Germany). The NMR spectrometer was operated with XWINNMR 3.6 (Bruker Biospin AG, Fällanden, Switzerland)

Chromatographic conditions: 10 μL injections of a 1.9 mg mL⁻¹ solution were made at 25 °C into a 150 mm \times 3.0 mm Zorbax SB C18 3 μm HPLC column maintained in an oven at 30 °C. The column was eluted at a flow rate of 0.5 mL min⁻¹; mobile phase A consisted of 0.1% formic acid, and mobile phase B consisted of acetonitrile. A gradient elution started with 75% A for 3 min was linearly increased to 95% B in 12 min and maintained at 95% B for 4 min, returned to 75% A over 1 min, and then re-equilibrated over a final 5 min prior to injection of the next sample. The mass spectrometer was operated in positive mode with a dry gas flow of 6 L min⁻¹, nebulizer pressure of 19 psi, and dry temperature of 305 °C. The MS instrument was set to acquire over the mass range m/z 50–800.

SPE: For solid phase extraction general purpose Hysphere Resin GP (10 mm \times 2 mm, 10–12 μm), Spark Holland Emmen, Netherlands) were preconditioned with 1 mL acetonitrile and 1 mL water respectively. The make up pump was set to a flow rate of 2 mL water.

NMR: Structure elucidation of the metabolites was performed on a Bruker AV 600 spectrometer equipped with an 5 mm TCI cryo probe. First a standard 1D proton spectrum was acquired. For this 40000 data points were collected with 128 transients, an acquisition time of 2 s and a spectral width of 10000 Hz. Between each

transient a delay of 1.5 s was set. Exponential line broadening of 0.5 Hz was applied prior to Fourier transformation. The total experiment time amounted to 7 min 51 s.

For structure elucidation a 2D standard TOCSY^[11] pulse sequence from the vendor-supplied library was employed. 128 t1 increments with four transients and 1024 complex data points were acquired with a spectral width of 1001 Hz in f2 and in f1, respectively. The TOCSY mixing time was set to 120 ms and the interscan delay to 2.5 s. The total acquisition time was 27 min and 59 s. The data were treated with a shifted ($\pi/2$) squared sine bell window function in both dimensions and zero-filled in f1 dimension to 256 data points.

In addition a NOESY^[11] experiment was performed using a standard pulse sequence of the vendor supplied library. Here, 256 t1 increments with 40 transients and 2048 complex data points were acquired with a spectral width of 5001 Hz in f2 and in f1, respectively. The mixing time was set to 1.5 s and the inter scan delay to 3 s. The total acquisition time amounts to 13 h and 34 min. The data were treated with a shifted ($\pi/2$) squared sine bell window function in both dimensions and zero-filled in f1 dimension to 512 data points.

Full experimental details for the preparation and characterization of **1–3** and **20–24** are provided in the Supporting Information.

Keywords: analytical methods · biotransformation · LC-SPE-NMR-MS · metabolism · mGlu5 receptor

- [1] a) Y. Chen, M. Monshouwer, W. L. Fitch, *Pharm. Res.* **2007**, *24*, 248–257; b) A.-E. F. Nassar, R. E. Talaat, *Drug Discovery Today* **2004**, *9*, 317–327.
- [2] a) M. Sandvoss, B. Bardsley, T. L. Beck, E. Lee-Smith, S. E. North, P. J. Moore, A. J. Edwards, R. J. Smith, *Magn. Reson. Chem.* **2005**, *43*, 762–770; b) O. Corcoran, M. Spraul, *Drug Discovery Today* **2003**, *8*, 624–631; c) N. T. Nyberg, H. Baumann, L. Kenne, *Magn. Reson. Chem.* **2001**, *39*, 236–240; d) B. Kammerer, H. Scheible, G. Zurek, M. Godejohann, K.-P. Zeller, C. H. Gleiter, W. Albrecht, S. Laufer, *Xenobiotica* **2007**, *37*, 280–297; e) M. Godejohann, L. H. Tseng, U. Braumann, J. Fuchser, M. Spraul, *J. Chromatogr. A* **2004**, *1058*, 191–196; f) V. Exarchou, M. Godejohann, T. A. van Beek, I. P. Gerothanassis, J. Vervoort, *Anal. Chem.* **2003**, *75*, 6288–6294.
- [3] N. P. Vasilev, M. K. Julsing, A. Koulman, C. Clarkson, H. J. Woerdenbag, I. Ionkova, R. Bos, J. W. Jaroszewski, O. Kayser, W. J. Quax, *J. Biotechnol.* **2006**, *126*, 383–393.
- [4] P. Bach, M. Isaac, A. Slassi, *Expert Opin. Ther. Pat.* **2007**, *17*, 371–384.
- [5] a) W. P. J. M. Spooren, F. Gasparini, T. E. Salt, R. Kuhn, *Trends Pharmacol. Sci.* **2001**, *22*, 331; b) T. M. Ballard, M. L. Woolley, E. Prinssen, J. Huwyler, R. Porter, W. Spooren, *Psychopharmacology* **2005**, *179*, 218–229.
- [6] B. Buettelmann, S. M. Ceccarelli, G. Jaeschke, S. Kolczewski, R. H. P. Porter, E. Vieira, PCT Int. Appl. WO 2006074884, **2006**.
- [7] N. J. Clarke, D. Rindgen, W. A. Korfmacher, K. A. Cox, *Anal. Chem.* **2001**, *73*, 430A–439A.
- [8] a) T. Friedberg, M. P. Pritchard, M. Bandera, S. P. Hanlon, D. Yao, L. A. McLaughlin, S. Ding, B. Burchell, C. R. Wolf, *Drug Metabolism* **1999**, *31*, 523–544; b) E. M. J. Gillam, T. Baba, B. R. Kim, S. Ohmori, F. P. Guengerich, *Arch. Biochem. Biophys.* **1993**, *305*, 123–131.
- [9] B. Golankiewicz, P. Januszczyk, M. Gdaniec, Z. Kosturkiewicz, *Tetrahedron* **1985**, *41*, 5989–5994.
- [10] T. Omura, R. Sato, *J. Biol. Chem.* **1964**, *239*, 2370–2378.
- [11] a) A. Bax, D. G. Davis, *J. Magn. Reson.* **1985**, *65*, 355–360; b) A. Kumar, R. R. Ernst, K. Wüthrich, *Biochem. Biophys. Res. Commun.* **1980**, *95*, 1–6.

Received: August 8, 2007

Revised: September 24, 2007

Published online on November 12, 2007